ELSEVIER

International Journal of Solids and Structures 40 (2003) 7425–7448

INTERNATIONAL JOURNAL OF SOLIDS and STRUCTURES

www.elsevier.com/locate/ijsolstr

Out-of-plane responses of a circular curved Timoshenko beam due to a moving load

Jong-Shyong Wu *, Lieh-Kwang Chiang

Department of Naval Architecture and Marine Engineering, National Chen-Kung University, Tainan 701, Taiwan, ROC

Received 14 March 2003

Abstract

For the cases of using the finite curved beam elements and taking the effects of both the shear deformation and rotary inertias into consideration, the literature regarding either free or forced vibration analysis of the curved beams is rare. Thus, this paper tries to determine the dynamic responses of a circular curved Timoshenko beam due to a moving load using the curved beam elements. By taking account of the effect of shear deformation and that of rotary inertias due to bending and torsional vibrations, the stiffness matrix and the mass matrix of the curved beam element were obtained from the force–displacement relations and the kinetic energy equations, respectively. Since all the element property matrices for the curved beam element are derived based on the local polar coordinate system (rather than the local Cartesian one), their coefficients are invariant for any curved beam element with constant radius of curvature and subtended angle and one does not need to transform the property matrices of each curved beam element from the local coordinate system to the global one to achieve the overall property matrices for the entire curved beam structure before they are assembled. The availability of the presented approach has been verified by both the existing analytical solutions for the entire continuum curved beam and the numerical solutions for the entire discretized curved beam composed of the conventional straight beam elements based on either the consistent-mass model or the lumped-mass model. In addition to the typical circular curved beams, a hybrid curved beam composed of one curved-beam segment and two identical straight-beam segments subjected to a moving load was also studied. Influence on the dynamic responses of the curved beams of the slenderness ratio, moving-load speed, shear deformation and rotary inertias was investigated.

Keywords: Curved beam element; Shear deformation; Rotary inertia; Finite element method; Moving load; Dynamic response

1. Introduction

Although the curved beam is used extensively in structures, the works using the finite curved beam elements to analyze either in-plane or out-of-plane vibrations of curved beams are still quite limited. The main reason for the last situation is that the complex formulations for the existing element property matrices of

* Corresponding author. Fax: +886-6-2747019/280-8458.
E-mail address: jswu@mail.ncku.edu.tw (J.-S. Wu).

0020-7683/$ - see front matter © 2003 Elsevier Ltd. All rights reserved.
doi:10.1016/j.ijsolstr.2003.07.004

the curved beam element discourage the engineers from employing it. Therefore, this paper tries to look for the more simple approach to tackle to the title problem.

In the pioneering works studying the out-of-plane vibrations of curved beams, both the analytical methods (Rao, 1971; Silva and Urgueira, 1988; Kirkhope, 1976; Wang et al., 1980; Bickford and Maganty, 1986; Kawakami et al., 1995; Yang and Wu, 2001; Lee et al., 2002) and the finite element methods (Davis et al., 1972a; Chaudhuri and Shore, 1977; Yoo and Fehrenbach, 1981; Palaninathan and Chandrasekharan, 1985; Lebeck and Knowlton, 1985; Howson and Jemah, 1999) were employed, but the analytical methods seem more popular. For the analytical methods, earlier studies were based on the classical beam theory with the effects of shear deformation and/or rotary inertias neglected until Rao (1971), Kirkhope (1976), Silva and Urgueira (1988) presented the more accurate models. By taking into account of the effects of shear deformation and rotary inertias, Rao (1971) used the Hamilton's principle to derive the differential equations for the coupled bending and torsional vibration of a curved beam and solved for the natural frequencies of the circular rings and arcs. Based on the force/moment-displacement relationships presented by Rao (1971), Kirkhope (1976) and Silva and Urgueira (1988) derived the dynamic stiffness matrices for the out-of-plane vibration of the curved beams using the Lagrange's equations and the dynamic equilibrium equations, respectively, and then solved for the natural frequencies. Wang et al. (1980) have derived the general dynamic slope-deflection equations for the horizontally circular curved members and then used the conditions of dynamic equilibrium at each supporting joint to establish the frequency equation for the multi-span circular curved beam, where the circumferential forces in the curved beam were neglected. Bickford and Maganty (1986) have used the formulation like that of Rao (1971) to determine the natural frequencies of thick rings and found that the accuracy of the numerical results may be improved if the effect of variation in curvature across the cross-section of the thick curved beam was considered. Kawakami et al. (1995) have derived the characteristic equation by applying the discrete Green functions and using the numerical integration to obtain the eigenvalues for both the in-plane and out-of-plane free vibrations of the non-uniform curved beams, where the formulation is much complicated than that of the classical approaches. Yang and Wu (2001) have derived the analytical solutions for a horizontally curved beam subjected to vertical loads due to the gravities of the vehicles and horizontal loads due to the centrifugal forces of the vehicles moving along a circular path, and for simplicity, they neglected the effect of shear deformation and considered only the first mode approximations for the vertical defection and torsional angle in the forced vibration analysis. By considering the reactive forces and moments due to the elastic foundation, Lee et al. (2002) have derived the governing differential equations for the out-of-plane free vibration of the circular curved Timoshenko beams and solved for the natural frequencies numerically.

For the finite element methods, Davis et al. (1972a) have derived the element stiffness and mass matrices for the out-of-plane coupled bending and torsional vibration of curved Timoshenko beams from the force/moment-displacement relations and kinetic energy equations, respectively. Where all the element property matrices are derived based on the local straight-beam (Cartesian) coordinate system (rather than the local curvilinear (polar) coordinate system), thus, transforming each element property matrix for the local coordinate system to the one for the common global coordinate system is always required before it is assembled even if the radius of curvature for the entire curved beam is a constant. Chaudhuri and Shore (1977) have idealized the entire curved I-girder bridge as a structural system composed of three major components, roadway, slab and steel girders, and then discretized the three components by using the annular plate elements, the thin-walled circularly curved beam elements and the straight beam elements, respectively, where the warping effect of cross-section was considered but the shear deformation effect was neglected. Yoo and Fehrenbach (1981) have derived the stiffness and mass matrices of the spatial curved beam element by using the minimum potential energy theory, where the effects of warping and rotary inertias due to flexure and torsion were considered but shear deformation effect was neglected. Palaninathan and Chandrasekharan (1985) have derived the element stiffness matrix for a three-dimensional curved Timoshenko beam using the Castigliano's theorem, where the coupling effects between the normal and

transverse shear forces were considered and the element stiffness matrix was also derived in terms of the local straight-beam coordinates like that of Davis et al. (1972a,b). In the same year, by neglecting the effect of shear deformation, Lebeck and Knowlton (1985) also developed an element stiffness matrix for the three-dimensional curved beam using the ring theory, where the in-plane motions were coupled with the out-of-plane motions due to the unsymmetrical cross-sectional area and the element stiffness matrix was derived in terms of the local polar coordinates so that no coordinate transformation was needed to assemble the elements. Although the procedures for deriving the stiffness matrix of the curved beam element adopted by Lebeck and Knowlton (1985) are similar to those adopted by Chaudhuri and Shore (1977), the displacement functions obtained by Lebeck and Knowlton (1985) are much simpler than those by Chaudhuri and Shore (1977). Instead of the conventional element mass and stiffness matrices, Howson and Jemah (1999) have developed the exact frequency-dependent dynamic stiffness matrix for a curved beam element from the governing differential equations of motion and then used the standard assembling technique to construct the overall dynamic stiffness matrix for the entire curved beam to obtain the natural frequencies. Their approach has the advantage of achieving more accurate natural frequencies, but the solution procedure is complex and the associated mode shapes must be retrieved by any other reliable methods.

In the past three decades, some novel approaches for the curved beam elements have been presented, but they were not widely adopted in the practical applications because of their complexity or tediousness. To improve the complex formulations of the exiting approaches, this paper derived the stiffness matrix and mass matrix of the curved beam element from the force–displacement relations and the kinetic energy equations, respectively, where all the element property matrices were in terms of the local polar (curvilinear) coordinates (instead of the local Cartesian coordinates) with the effects of both shear deformation and rotary inertias considered. Comparing with the existing approaches (Davis et al., 1972a; Chaudhuri and Shore, 1977; Yoo and Fehrenbach, 1981; Palaninathan and Chandrasekharan, 1985), the present one has the following merits: (i) Instead of the local Cartesian (straight-beam) coordinate system, the element property matrices of this paper are derived in terms of the local polar (curvilinear) coordinates, so that, for a circular curved beam with constant radius of curvature, one may obtain the overall property matrices by directly assembling, and the coordinate transformation as done by Davis et al. (1972a), Chaudhuri and Shore (1977), Yoo and Fehrenbach (1981), and Palaninathan and Chandrasekharan (1985) is not required. (ii) For the hybrid structural systems composed of curved beam elements and straight beam elements, only one transformation from the local polar coordinate system to the global Cartesian coordinate system is required in this paper. However, two transformations are required for the techniques presented by Davis et al. (1972a), Chaudhuri and Shore (1977), Yoo and Fehrenbach (1981), and Palaninathan and Chandrasekharan (1985): the first transformation is from the local polar coordinate system to the local Cartesian coordinate system and the second transformation is from the local Cartesian coordinate system to the global Cartesian coordinate system. (iii) The sign convention for the nodal forces is identical to that for the nodal displacements, thus the transformation matrix for the nodal forces is the same as that for the nodal displacements. However, this is not true for the transformation matrices of Davis et al. (1972a,b), where the sign convention for the nodal forces is different from that for the nodal displacements. Although the procedure of deriving the element property matrices in this paper was similar to that of deriving the element stiffness matrix by Lebeck and Knowlton (1985), this paper considered the effect of shear deformation and also derived the element mass matrix and it was not true for the work of Lebeck and Knowlton (1985).

In this paper, the forced vibration responses of a horizontally curved beam subjected to a moving load were solved using the Newmark direct integration method (Bathe, 1982). Since, for the curved beams studied, the in-plane responses and the out-of-plane responses are uncoupled, the in-plane behaviors of the curved beam are neglected. In addition to the curved beam element and the consistent-mass model, the conventional straight beam element (Przemieniecki, 1968) and the lumped-mass model were also used to perform the free and forced vibration analyses of the curved beams. It is believed that good agreements

between the results obtained from different beam elements and different mass models will also be the reasonable evidence for the availability of the presented approach.

2. Displacement functions and shape functions

For an infinitesimal element of curved beam in static equilibrium as shown in Fig. 1, if each cross-section remains constant along the entire beam length and is doubly symmetric, then the displacement functions for the transverse displacement in the axial y-direction, u_y, the rotational (bending) angle about the radial x-axis, ψ_x, and the torsional (twisting) angle about the tangential z-axis, ψ_θ, are given by Lebeck and Knowlton (1985)

$$u_y = G_1 + G_2 C_{so}\theta + G_3 \sin\theta + G_4 \cos\theta + G_5 \theta \sin\theta + G_6 \theta \cos\theta \tag{1a}$$

$$\psi_x = \frac{1}{R}[G_2 + G_3 \cos\theta - G_4 \sin\theta + G_5(\theta\cos\theta + \sin\theta) - G_6(\theta \sin\theta - \cos\theta)] \tag{1b}$$

$$\psi_\theta = \frac{1}{R}[-G_3 \sin\theta - G_4 \cos\theta - G_5(\theta \sin\theta - 2C_o \cos\theta) - G_6(\theta\cos\theta + 2C_o \sin\theta)] \tag{1c}$$

where

$$C_o = \Phi_{bt}/(1 + \Phi_{bt}) \tag{2a}$$

$$C_{so} = 1 + [GJ_\theta/(R^2 k' GA)] \tag{2b}$$

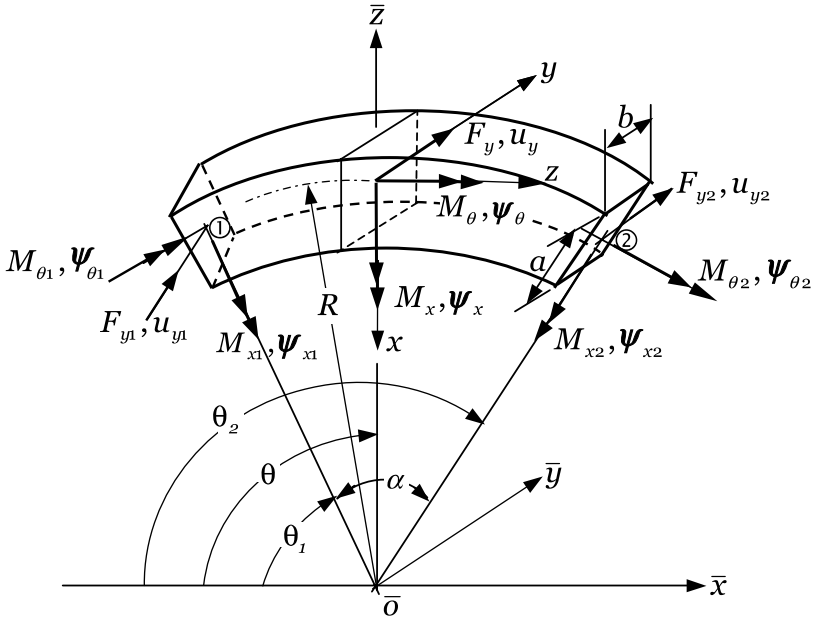

Fig. 1. The definition for the out-of-plane element forces (F_y, M_x and M_θ) and element displacements (u_y, ψ_x and ψ_θ) for a curved beam element with subtended angle α, the local curvilinear (polar) coordinate system $xyz(\theta)$ and the global coordinate system $\bar{x}\bar{y}\bar{z}$.

with

$$\Phi_{bt} = EI_x/(GJ_\theta) \tag{3a}$$

$$I_x = \int_A \frac{y^2}{1-(x/R)}\,\mathrm{d}A \tag{3b}$$

$$J_\theta = \int_A \frac{x^2+y^2}{1-(x/R)}\,\mathrm{d}A \tag{3c}$$

It is noted that the displacement functions given by Eqs. (1a)–(1c) are obtained from Lebeck and Knowlton (1985), but the shear deformation parameter $GJ_\theta/(R^2k'GA)$ appearing in Eq. (2b) is obtained from Davis et al. (1972a), because the effect of shear deformation is not considered by Lebeck and Knowlton (1985). In other words, the element displacements, u_y, ψ_x and ψ_θ, given by Eqs. (1a)–(1c) are the results of taking account of the effects of both shear deformation and rotary inertias and are available for either thin or thick curved beams.

In Eqs. (1a)–(1c), G_1–G_6 are the integration constants determined by the boundary conditions of the curved beam element, while in Eqs. (2) and (3), A is the cross-sectional area, R is the average radius of curvature of the curved beam element, I_x is the moment of inertia of the area A about the radial x-axis, J_θ is the polar moment of inertia of the area A about the tangential z-axis, E is the Young's modulus, G is the shear modulus and k' is the shear correction factor. The parameter Φ_{bt} defined by Eq. (3a) denotes the ratio of bending rigidity to torsional rigidity.

Rewriting Eqs. (1a)–(1c) in matrix form gives

$$\{u\} = [H]\{G\} \tag{4}$$

where

$$\{u\} = \{\, u_y \quad \psi_x \quad \psi_\theta \,\} \tag{5}$$

$$\{G\} = \{\, G_1 \quad G_2 \quad G_3 \quad G_4 \quad G_5 \quad G_6 \,\} \tag{6}$$

$$[H] = \begin{bmatrix} 1 & C_{\mathrm{so}}\theta & \sin\theta & \cos\theta & \theta\sin\theta & \theta\cos\theta \\ 0 & 1/R & \cos\theta/R & -\sin\theta/R & (\theta\cos\theta+\sin\theta)/R & -(\theta\sin\theta-\cos\theta)/R \\ 0 & 0 & -\sin\theta/R & -\cos\theta/R & -(\theta\sin\theta-2C_{\mathrm{o}}\cos\theta)/R & -(\theta\cos\theta+2C_{\mathrm{o}}\sin\theta)/R \end{bmatrix} \tag{7}$$

In Eqs. (4)–(7), the symbols $[\cdot]$ and $\{\cdot\}$ represent the rectangular (or square) matrix and the column vector, respectively.

Applying the boundary conditions for the curved beam element shown in Fig. 1 to Eq. (4), one obtains

$$\{\delta\} = [B]\{G\} \tag{8}$$

where

$$\{\delta\} = \{\, u_{y1} \quad \psi_{x1} \quad \psi_{\theta1} \quad u_{y2} \quad \psi_{x2} \quad \psi_{\theta2} \,\} \tag{9}$$

$$[B] = \left[\begin{array}{ccc:ccc} 1 & C_{so}\theta_1 & \sin\theta_1 & \cos\theta_1 & \theta_1\sin\theta_1 & \theta_1\cos\theta_1 \\ 0 & 1/R & \cos\theta_1/R & -\sin\theta_1/R & (\theta_1\cos\theta_1+\sin\theta_1)/R & -(\theta_1\sin\theta_1-\cos\theta_1)/R \\ 0 & 0 & -\sin\theta_1/R & -\cos\theta_1/R & -(\theta_1\sin\theta_1-2C_o\cos\theta_1)/R & -(\theta_1\cos\theta_1+2C_o\sin\theta_1)/R \\ \hdashline 1 & C_{so}\theta_2 & \sin\theta_2 & \cos\theta_2 & \theta_2\sin\theta_2 & \theta_2\cos\theta_2 \\ 0 & 1/R & \cos\theta_2/R & -\sin\theta_2/R & (\theta_2\cos\theta_2+\sin\theta_2)/R & -(\theta_2\sin\theta_2-\cos\theta_2)/R \\ 0 & 0 & -\sin\theta_2/R & -\cos\theta_2/R & -(\theta_2\sin\theta_2-2C_o\cos\theta_2)/R & -(\theta_2\cos\theta_2+2C_o\sin\theta_2)/R \end{array}\right] \tag{10}$$

From Eq. (8) one obtains the integration constants to be

$$\{G\} = [B]^{-1}\{\delta\} \tag{11}$$

The substitution of Eq. (11) into Eq. (4) determines the displacement function vector

$$\{u\} = [H][B]^{-1}\{\delta\} \tag{12}$$

According to the definition for the shape functions, from Eq. (12) one obtains

$$[\tilde{a}] = [H][B]^{-1} = \begin{bmatrix} \tilde{a}_{y1} & \tilde{a}_{y2} & \cdots & \tilde{a}_{y6} \\ \tilde{a}_{x1} & \tilde{a}_{x2} & \cdots & \tilde{a}_{x6} \\ \tilde{a}_{z1} & \tilde{a}_{z2} & \cdots & \tilde{a}_{z6} \end{bmatrix} \tag{13}$$

where the coefficients of $[\tilde{a}]$, $\tilde{a}_{yi}$, $\tilde{a}_{xi}$ and $\tilde{a}_{zi}$ ($i = 1$–6), appearing in Eq. (13) denote the shape functions associated with deflections in y, x and z directions, u_y, ψ_x and ψ_θ, respectively. For simplicity, "implicit" shape functions $[\tilde{a}]$, instead of the "explicit" ones, were used in this paper.

3. Stiffness matrix for curved beam element

From Davis et al. (1972a,b) and Lebeck and Knowlton (1985) one obtains the following force–displacement relations

$$F_y = \frac{k'GA}{R}(u_y' - R\psi_x) \tag{14a}$$

$$M_x = \frac{EI_x}{R^2}(u_y'' - R\psi_\theta) \tag{14b}$$

$$M_\theta = \frac{GJ_\theta}{R^2}(R\psi_\theta' + R\psi_x) \tag{14c}$$

where the primes denote the derivatives with respect to the angular coordinate θ.

From Eqs. (1) and (14) one obtains

$$\{f\} = [d]\{G\} \tag{15}$$

where

$$\{f\} = \{\, F_y \quad M_x \quad M_\theta \,\} \tag{16}$$

$$[d] = \frac{EI_x}{R^2}\begin{bmatrix} 0 & 1/(R\Phi_{bt}) & 0 & 0 & 0 & 0 \\ 0 & 0 & 0 & 0 & 2\cos\theta/(1+\Phi_{bt}) & -2\sin\theta/(1+\Phi_{bt}) \\ 0 & 1/\Phi_{bt} & 0 & 0 & -2\sin\theta/(1+\Phi_{bt}) & -2\cos\theta/(1+\Phi_{bt}) \end{bmatrix} \tag{17}$$

Static equilibrium between the forces at node ① and those at node ② for the curved beam element shown in Fig. 1 requires that

$$\{\, F_{y1} \quad M_{x1} \quad M_{\theta 1} \,\} = -\{\, F_{y2} \quad M_{x2} \quad M_{\theta 2} \,\} \tag{18}$$

Applying Eq. (15) to node ① and node ② (see Fig. 1) and using the relations given by Eq. (18), one obtains

$$\{F\} = [D]\{G\} \tag{19}$$

where

$$\{F\} = \{\, F_{y1} \quad M_{x1} \quad M_{\theta 1} \quad F_{y2} \quad M_{x2} \quad M_{\theta 2} \,\} \tag{20}$$

$$[D] = \frac{EI_x}{R^2} \left[\begin{array}{ccc:ccc} 0 & -1/(R\Phi_{bt}) & 0 & 0 & 0 & 0 \\ 0 & 0 & 0 & 0 & -2\cos\theta_1/(1+\Phi_{bt}) & 2\sin\theta_1/(1+\Phi_{bt}) \\ 0 & -1/\Phi_{bt} & 0 & 0 & 2\sin\theta_1/(1+\Phi_{bt}) & 2\cos\theta_1/(1+\Phi_{bt}) \\ \hdashline 0 & 1/(R\Phi_{bt}) & 0 & 0 & 0 & 0 \\ 0 & 0 & 0 & 0 & 2\cos\theta_2/(1+\Phi_{bt}) & -2\sin\theta_2/(1+\Phi_{bt}) \\ 0 & 1/\Phi_{bt} & 0 & 0 & -2\sin\theta_2/(1+\Phi_{bt}) & -2\cos\theta_2/(1+\Phi_{bt}) \end{array}\right] \tag{21}$$

Introducing the values of $\{G\}$ defined by Eq. (11) into Eq. (19) gives

$$\{F\} = [D][B]^{-1}\{\delta\} = [K]\{\delta\} \tag{22}$$

where

$$[K] = [D][B]^{-1} \tag{23}$$

represents the stiffness matrix of the curved beam element.

4. Mass matrix for curved beam element

For the curved beam element shown in Fig. 1, its kinetic energy is given by

$$T = \frac{1}{2}\int_{\theta_1}^{\theta_2} \rho\{\dot{u}\}^{\mathrm{T}}[\Lambda]\{\dot{u}\}R\,\mathrm{d}\theta \tag{24}$$

where

$$[\Lambda] = \begin{bmatrix} A & 0 & 0 \\ 0 & I_x & 0 \\ 0 & 0 & J_\theta \end{bmatrix} \tag{25}$$

In Eq. (24), the dots denote the derivatives with respect to time t and ρ is the mass density of the beam material, while in Eq. (25), the values of I_x and J_θ are defined by Eqs. (3b) and (3c), respectively.

For harmonic free vibrations, one has

$$\{u\} = \{\bar{u}\}\mathrm{e}^{\mathrm{i}\omega t} \tag{26}$$

where $\{\bar{u}\}$ is the amplitude of $\{u\}$, ω is the natural frequency of the curved beam, t is time and $\mathrm{i} = \sqrt{-1}$.

Substituting Eq. (26) into Eq. (24) and using the relation given by Eq. (12) yield

$$T = \frac{1}{2}\omega^2\{\delta\}^{\mathrm{T}}[M]\{\delta\} \tag{27}$$

where

$$[M] = \rho R([B]^{-1})^{\mathrm{T}}\left(\int_{\theta_1}^{\theta_2}[H]^{\mathrm{T}}[\Lambda][H]\,\mathrm{d}\theta\right)[B]^{-1} \tag{28}$$

denotes the "consistent mass matrix" of the curved beam element.

To determine the consistent mass matrix of a curved beam element, $[M]$, using Eq. (28), it is only required to calculate the following integration

$$[\overline{H}] = \int_{\theta_1}^{\theta_2} [H]^{\mathrm{T}} [\Lambda][H] \, \mathrm{d}\theta \tag{29}$$

and all the other numerical calculations are performed by computer. The results for the integration defined by Eq. (29) are shown in Appendix A at the end of this paper.

For comparison, a "lumped mass matrix" for the same curved beam element given by

$$[M^*] = \tfrac{1}{2}\rho R\alpha \lceil A I_x J_\theta A I_x J_\theta \rfloor \tag{30}$$

was also introduced. Where the symbol $\lceil \cdot \rfloor$ denotes a diagonal matrix and the notation α $(= \theta_2 - \theta_1)$ denotes the subtended angle of the curved beam element (see Fig. 1).

5. Property matrices and shape functions for straight beam element

Since all the element stiffness and mass matrices for the straight beam element given by Przemieniecki (1968) were derived based on the local coordinate system, *xyz*, shown in Fig. 2(a) and part of them is available only for a two-dimensional beam, how to use the materials of the existing literature to incorporate with the property matrices established on the local curvilinear coordinate system for the curved beam element, $xyz(\theta)$, shown in Fig. 2(b) is the key point of using the straight beam element to tackle the title problem. In Fig. 2(a) the longitudinal axis along the length of the straight beam is selected as the *x*-axis, but in Fig. 2(b) the circumferential axis along the length of the curved beam is selected as the *z*-axis (or θ-axis, cf. Fig. 1). Since both the coordinate systems shown in Fig. 2(a) and (b) obey the right-hand rule and the positive directions for the two *y*-axes are assumed to be identical here, the positive *x*-axis for the coordinate system shown in Fig. 2(b) must be opposite to the positive *z*-axis for the coordinate system shown in Fig. 2(a). For this reason, the coefficients of the element property matrices in terms of the coordinate of Fig. 2(b) and relating to *z*, *y* and *x* are equal to the associated ones of Przemieniecki (1968) relating to *x*, *y* and *z*, respectively. In other words, some of the sequential order and the sign convention for the coefficients of the element property matrices derived based on the coordinate system shown in Fig. 2(a) (Przemieniecki, 1968) must be changed, then the results obtained may agree with the corresponding ones derived based on the curvilinear coordinate system shown in Fig. 2(b). By means of the foregoing technique and by referring to Przemieniecki (1968) one may obtain the stiffness and mass matrices of the straight Timoshenko beam

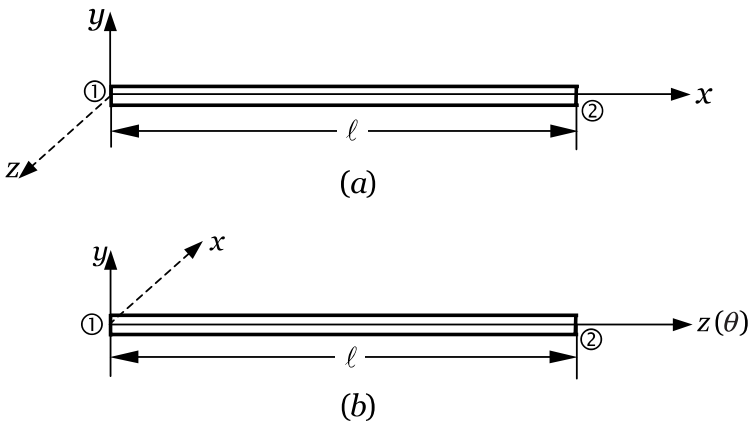

Fig. 2. (a) The local coordinate system for the conventional straight beam element (Przemieniecki, 1968), *xyz*, and (b) the local curvilinear coordinate system for the curved beam element in this paper, $xyz(\theta)$.

element as shown in the report of Wu and Chiang (2003) and the associated shape functions given by (cf. Fig. 2(b))

$$[\bar{a}]^{\mathrm{T}} = \begin{bmatrix} \bar{a}_{y1} & \bar{a}_{y2} & \cdots & \bar{a}_{y6} \\ \bar{a}_{x1} & \bar{a}_{x2} & \cdots & \bar{a}_{x6} \\ \bar{a}_{z1} & \bar{a}_{z2} & \cdots & \bar{a}_{z6} \end{bmatrix}^{\mathrm{T}}$$

$$= \begin{bmatrix} C_{sy}[1-3\xi^2+2\xi^3+(1-\xi)\Phi_y] & C_{sy}(6\xi-6\xi^2)\eta & 0 \\ -C_{sy}[\xi-2\xi^2+\xi^3+\frac{1}{2}(\xi-\xi^2)\Phi_y]\ell & -C_{sy}[-1+4\xi-3\xi^2-(1-\xi)\Phi_y]\ell\eta & 0 \\ -(1-\xi)\ell\zeta & 0 & -(1-\xi)\ell\eta \\ C_{sy}(3\xi^2-2\xi^3+\xi\Phi_y) & C_{sy}(-6\xi+6\xi^2)\eta & 0 \\ -C_{sy}[-\xi^2+\xi^3-\frac{1}{2}(\xi-\xi^2)\Phi_y]\ell & -C_{sy}(2\xi-3\xi^2-\xi\Phi_y)\ell\eta & 0 \\ -\ell\xi\zeta & 0 & -\ell\xi\eta \end{bmatrix} \tag{31}$$

where

$$\xi = \frac{z}{\ell}, \quad \eta = \frac{y}{\ell}, \quad \zeta = \frac{x}{\ell} \tag{32a}$$

$$C_{sy} = 1/(1+\Phi_y) \tag{32b}$$

$$\Phi_y = 12EI_x/(k'GA\ell^2) \tag{32c}$$

It is noted that, for the case of considering the effect of shear deformation, Przemieniecki (1968) only gives the shape functions relating to the transverse deflections (u_y) and rotation (ψ_x) of a two-dimensional beam element, i.e., $\bar{a}_{yi}$ and $\bar{a}_{xi}$ ($i = 1, 2, 4, 5$), and all the other shape functions appearing Eq. (31) were derived by this paper. It will be also noted that the (positive and negative) signs of the eight shape functions given by Przemieniecki (1968), $\bar{a}_{yi}$ and $\bar{a}_{xi}$ ($i = 1, 2, 4, 5$), are not exactly identical to those shown in Eq. (31) because of the reason shown in the first paragraph of this section (cf. Fig. 2).

6. External loading vector due to a moving load

For a horizontally curved beam subjected to a moving load with magnitude P along the circumferential direction, all nodal forces of the whole curved beam are equal to zero except those of the beam element on which the moving load P applies. The non-zero elemental nodal force vector is given by

$$\{F\} = \{a_y\}P \tag{33}$$

where

$$\{F\} = \{\, F_{y1} \quad M_{x1} \quad M_{\theta 1} \quad F_{y2} \quad M_{x2} \quad M_{\theta 2} \,\} \tag{34}$$

$$\{a_y\} = \{\, \tilde{a}_{y1}(\theta) \quad \tilde{a}_{y2}(\theta) \quad \cdots \quad \tilde{a}_{y6}(\theta) \,\} \text{ (for curved beam elements)} \tag{35a}$$

$$\{a_y\} = \{\, \bar{a}_{y1}(\xi) \quad \bar{a}_{y2}(\xi) \quad \cdots \quad \bar{a}_{y6}(\xi) \,\} \text{ (for straight beam elements)} \tag{35b}$$

In Eq. (35a) the values of $\tilde{a}_{yi}(\theta)$ ($i = 1$–6) denote the shape functions for the "curved" beam element defined by Eq. (13), and in Eq. (35b) the values of $\bar{a}_{yi}(\xi)$ ($i = 1$–6) denote the shape functions for the "straight" beam element defined by the first column of Eq. (31).

7. Transformation from local to global coordinate system

The stiffness matrix and mass matrix for the curved beam element derived in the previous sections are in terms of the local curvilinear (polar) coordinate system, $xyz(\theta)$. Direct assemblage of all the element property matrices will determine the overall property matrices for the entire circular curved beam with constant radius of curvature and transforming each element property matrix from the local coordinates to the global ones is not required before assemblage. But this is not true for the element property matrices of the curved beam element derived in by Davis et al. (1972a), Chaudhuri and Shore (1977), Yoo and Fehrenbach (1981), and Palaninathan and Chandrasekharan (1985), because they are derived in terms of the local Cartesian coordinates $\tilde{x}\tilde{y}\tilde{z}$ as shown in Fig. 3 or 4. However, if a curved beam is composed of many curved beam segments with different curvatures or is discretized by many straight beam elements, then transformation of each property matrix for either the curved beam element or the straight beam element is always required before it is assembled.

7.1. Transformation matrix for the curved beam element

For the curved beam element shown in Fig. 3, if the nodal displacements with respect to the local curvilinear (polar) coordinate system $xyz(\theta)$ are represented by

$$\{\delta\} = \{\, u_{y1} \quad \psi_{x1} \quad \psi_{\theta 1} \quad u_{y2} \quad \psi_{x2} \quad \psi_{\theta 2} \,\} \tag{36}$$

and those with respect to the global coordinate system $\bar{x}\bar{y}\bar{z}$ are represented by

$$\{\bar{\delta}\} = \{\, \bar{u}_1 \quad \bar{u}_2 \quad \bar{u}_3 \quad \bar{u}_4 \quad \bar{u}_5 \quad \bar{u}_6 \,\} \tag{37}$$

then the relationship between $\{\delta\}$ and $\{\bar{\delta}\}$ is given by

$$\{\delta\} = [\lambda]\{\bar{\delta}\} \tag{38}$$

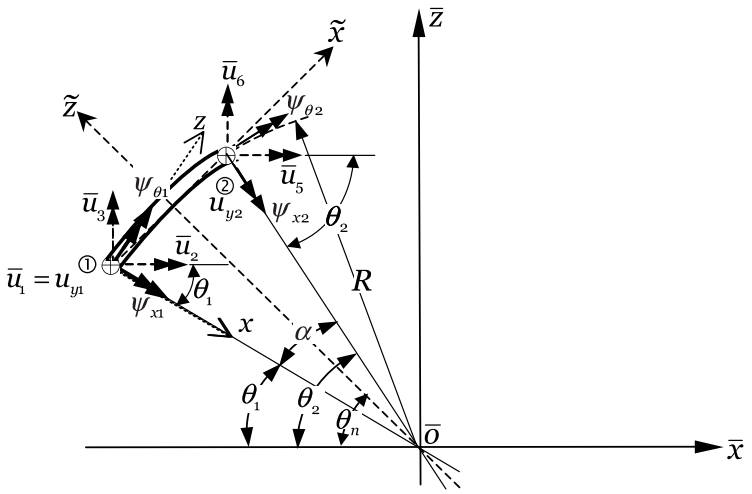

Fig. 3. The relationship between the nodal displacements for the curved beam element in the local curvilinear coordinate system $xyz(\theta)$, $u_{y1}, \psi_{x1}, \psi_{\theta 1}, \ldots, \psi_{\theta 2}$, and those in the global coordinate system $\bar{x}\bar{y}\bar{z}$, $\bar{u}_1, \bar{u}_2, \bar{u}_3, \ldots, \bar{u}_6$.

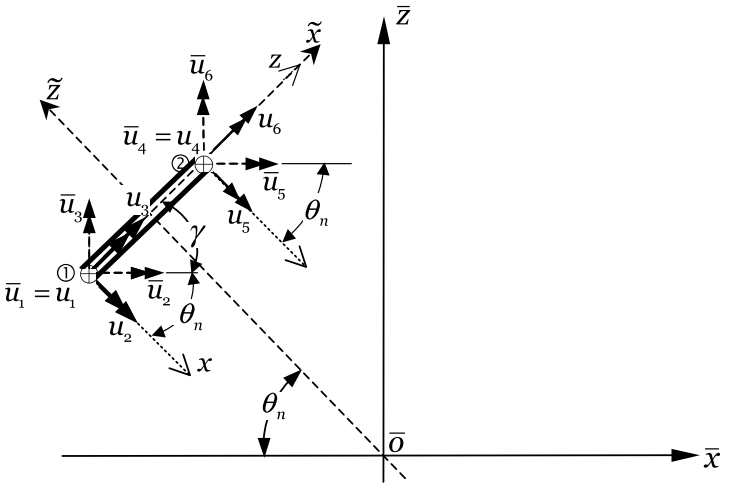

Fig. 4. The relationship between the nodal displacements for the straight beam element in the local Cartesian coordinate system, xyz, $u_1, u_2, u_3, \ldots, u_6$, and those in the global coordinate system $\bar{x}\bar{y}\bar{z}$, $\bar{u}_1, \bar{u}_2, \bar{u}_3, \ldots, \bar{u}_6$.

where

$$[\lambda] = \left[\begin{array}{ccc:ccc} 1 & 0 & 0 & 0 & 0 & 0 \\ 0 & \cos\theta_1 & -\sin\theta_1 & 0 & 0 & 0 \\ 0 & \sin\theta_1 & \cos\theta_1 & 0 & 0 & 0 \\ \hdashline 0 & 0 & 0 & 1 & 0 & 0 \\ 0 & 0 & 0 & 0 & \cos\theta_2 & -\sin\theta_2 \\ 0 & 0 & 0 & 0 & \sin\theta_2 & \cos\theta_2 \end{array}\right] \tag{39}$$

which is the transformation matrix for the element property matrices of the curved beam element derived in the previous sections. In Eq. (39), θ_1 denotes the angle between the negative $\bar{x}$-axis and the negative local curvilinear x-axis at node ① and θ_2 denotes that at node ② (see Fig. 3). They are measured as positive in the clockwise direction from the negative $\bar{x}$-axis.

Based on the transformation matrix given by Eq. (39), the stiffness and mass matrices of a curved beam element with respect to the global coordinate system $\bar{x}\bar{y}\bar{z}$, $[\overline{K}]$ and $[\overline{M}]$, are respectively determined by

$$[\overline{K}] = [\lambda]^{\mathrm{T}}[K][\lambda] \tag{40}$$

$$[\overline{M}] = [\lambda]^{\mathrm{T}}[M][\lambda] \tag{41}$$

where $[K]$ and $[M]$ are the stiffness and mass matrices of a curved beam element with respect to the local curvilinear coordinate system $xyz(\theta)$ defined by Eqs. (23) and (28), respectively. Eq. (41) is also available for the element lumped mass matrix $[M^*]$ defined by Eq. (30). It is noted that, in the existing literature of Davis et al. (1972a,b), Chaudhuri and Shore (1977), Yoo and Fehrenbach (1981) and Palaninathan and Chandrasekharan (1985), two transformations are required for the property matrices of each curved beam element before they are assembled: the first transformation is from the local curvilinear coordinate system $xyz(\theta)$ to the local Cartesian coordinate system $\tilde{x}\tilde{y}\tilde{z}$ (see Figs. 3 and 4) and the second transformation is from the local Cartesian coordinate system $\tilde{x}\tilde{y}\tilde{z}$ to the global coordinate system $\bar{x}\bar{y}\bar{z}$. However, the formulation of this paper requires only one transformation, because the property matrices of each curved beam element

are transformed directly from the local curvilinear coordinate system $xyz(\theta)$ to the global coordinate system $\bar{x}\bar{y}\bar{z}$ as one may see from Eqs. (40) and (41).

7.2. Transformation matrix for the straight beam element

Similarly, for the straight beam element shown in Fig. 4, if the nodal displacements with respect to the local Cartesian coordinate system xyz are represented by

$$\{\delta_s\} = \{u_1 \quad u_2 \quad u_3 \quad u_4 \quad u_5 \quad u_6\} \tag{42}$$

and those with respect to the global coordinate system $\bar{x}\bar{y}\bar{z}$ are represented by Eq. (37), then the relationship between $\{\delta_s\}$ and $\{\bar{\delta}\}$ is given by

$$\{\delta_s\} = [\lambda_s]\{\bar{\delta}\} \tag{43}$$

where

$$[\lambda_s] = \left[\begin{array}{ccc:ccc} 1 & 0 & 0 & 0 & 0 & 0 \\ 0 & \cos\theta_n & -\sin\theta_n & 0 & 0 & 0 \\ 0 & \sin\theta_n & \cos\theta_n & 0 & 0 & 0 \\ \hdashline 0 & 0 & 0 & 1 & 0 & 0 \\ 0 & 0 & 0 & 0 & \cos\theta_n & -\sin\theta_n \\ 0 & 0 & 0 & 0 & \sin\theta_n & \cos\theta_n \end{array}\right] \tag{44}$$

which is the transformation matrix for the element property matrices of the straight beam element. Where θ_n denotes the angles between the negative $\bar{x}$-axis and the outward "normal" for the straight beam element (i.e., the $\tilde{z}$-axis in Figs. 3 and 4). It is also measured as positive in the clockwise direction from the negative $\bar{x}$-axis. In general, the coefficients of the transformation matrix for a straight beam element are determined by the global coordinates of the two nodes (① and ②) of the beam elements, $(\bar{x}_1, \bar{y}_1, \bar{z}_1)$ and $(\bar{x}_2, \bar{y}_2, \bar{z}_2)$. In such a case, the angle θ_n is determined by (cf. Fig. 4)

$$\theta_n = 0.5\pi - \gamma \tag{45}$$

where γ is the angle between the straight beam element and the positive $\bar{x}$-axis given by

$$\gamma = \tan^{-1}[(\bar{z}_2 - \bar{z}_1)/(\bar{x}_2 - \bar{x}_1)] \tag{46}$$

8. Numerical results and discussions

For convenience, a curved beam with the effects of both rotary inertias and shear deformation neglected is call the "Euler" beam, the one with only the effect of rotary inertias due to bending and torsional vibrations considered is call the "rotary" beam, and the one with the effects of both rotary inertias and shear deformation considered is call the "Timoshenko" beam, in this paper. In addition, the total number of elements is $n_e = 20$ for the results obtained from the curved beam (CB) elements and $n_e = 40$ for those obtained from the straight beam (SB) elements (Wu and Chiang, 2003), and all the numerical results refer to those obtained from the Timoshenko beams using the curved beam (CB) elements incorporated with the consistent-mass models if there is no particular declaration.

8.1. Convergence of the presented method

In this section a circular curved Timoshenko beam with total subtended angle $\bar{\alpha} = 180°$ and clamped–clamped ends (i.e., $u_y = 0$, $\psi_x = 0$, $\psi_\theta = 0$ at $\theta = 0°$ and 180°) is used to show the convergence of the presented curved beam element. The other given data for the beam are: radial thickness $a = 2''$, axial thickness $b = 2''$, average radius of curvature $R = 4''$, $A = ab = 4$ in.^{2}, $I_x = 1.3622$ in.^{4}, $I_y = 1.3856$ in.^{4}, $J_\theta = I_x + I_y = 2.7478$ in.^{4}, Poisson's ratio $\upsilon = 0$, shear correction factor $k' = 0.833$, Young's modulus $E = 30 \times 10^6$ psi and shear modulus $G = E/[2(1+\upsilon)] = 15 \times 10^6$ psi. The four solid lines (—) in Fig. 5(a)–(d) show the relationships between the lowest four natural frequencies ($\tilde{\omega}_i$, $i = 1$–4) of the 180° clamped–clamped Timoshenko beam obtained from the presented method (based on consistent mass model) and the total number of curved beam elements used, n_e. The natural frequencies corresponding to the four horizontal dashed lines (– – – –) in Fig. 5(a)–(d) are the exact values obtained from Rao (1971). It is evident that the FEM results of this paper are very close to the exact values if $n_e > 20$ and this is the reason why 20 curved beam elements are used to do the finite element analysis in this paper.

8.2. Validation of natural frequencies

To confirm the reliability of the formulations of this paper, the last clamped–clamped circular curved beam with total subtended angles $\bar{\alpha} = 180°$, 270° and 360° is further studied. It is noted that the given data for the last curved beam are selected to be completely satisfied the conditions given by Tables 3–5 of Rao (1971): $EI_x/GJ_\theta = 1.0$, $E/G = 2.0$, $a/b = 1.0$ and $a/R = 0.5$, so that one may compare the current numerical results with the exact solutions of Rao (1971). For simplicity, the values of moment of inertias for the cross-sectional areas are usually calculated with the classical simple formulas (Kawakami et al., 1995, Yang and

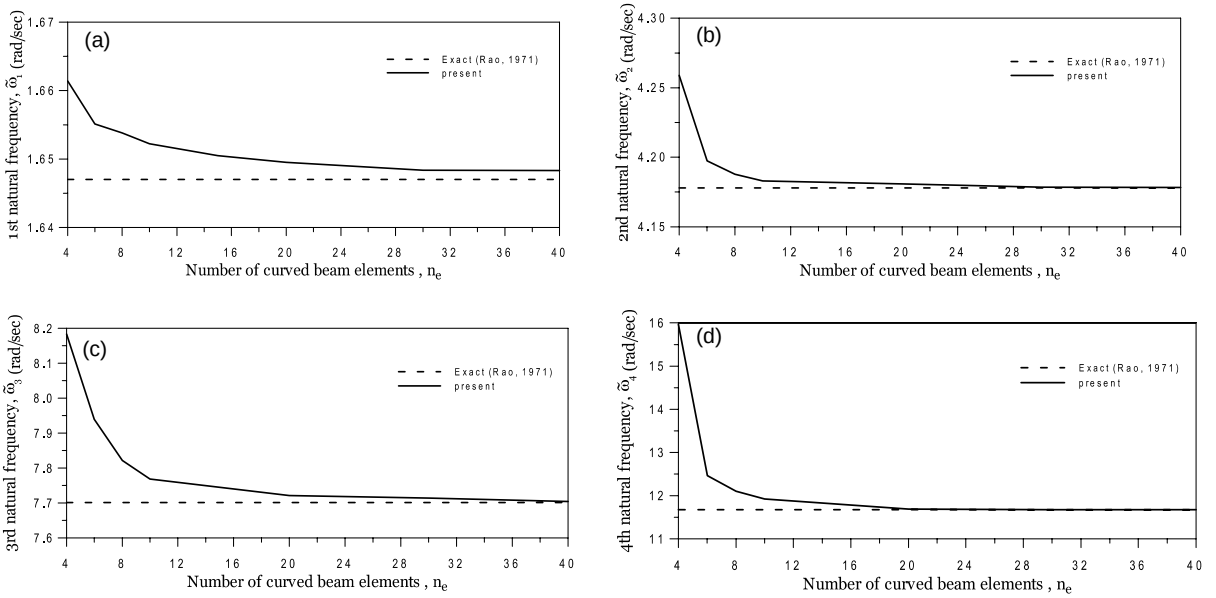

Fig. 5. The relationships between the lowest four natural frequencies ($\tilde{\omega}_i$, $i = 1$–4) of the 180° clamped–clamped Timoshenko beam and the total number of curved beam elements, n_e, for (a) $\tilde{\omega}_1$, (b) $\tilde{\omega}_2$, (c) $\tilde{\omega}_3$, and (d) $\tilde{\omega}_4$.

Wu, 2001; Lee et al., 2002), $I_x = ab^3/12$, $I_y = a^3b/12$ and $J_\theta = I_x + I_y$, rather than by the laborious formulas given by Eqs. (3b) and (3c). This is one of the main reasons that the numerical results of one report may be slightly different from those of the other report as shown by Davis et al. (1972b). Since the natural frequencies obtained with the values of I_x and J_θ defined by Eqs. (3b) and (3c) are more close to the exact values of Rao (1971), this paper uses Eqs. (3b) and (3c) to calculate the values of I_x and J_θ except those relating to Yang and Wu (2001).

Table 1(panel A) shows the influence of the total subtended angle $\bar{\alpha}$ and the slenderness ratio $\widetilde{S}_r = [b/(R\bar{\alpha})](b/R)$ on the lowest four frequency parameters of the circular Euler, rotary and Timoshenko curved beams, $\beta_i = \omega_i\sqrt{\rho AR^4/(EI_x)}$ ($i = 1$–4), based on the "consistent-mass" model, while Table 1(panel B) shows that based on the "lumped-mass" model. Where the symbols "$\sim$" and "_" on the top of the

Table 1
The lowest four natural-frequency parameters of the 180°, 270° and 360° circular arcs with fixed end conditions, $\beta_i = \omega_i\sqrt{\rho AR^4/(EI_x)}$ ($i = 1$–4), based on "consistent-mass" (panel A) and "lumped-mass" (panel B) models

$\bar{\alpha}$ ($\widetilde{S}_r$)	Mode no., i	Euler beam			Rotary beam			Timoshenko beam		
		Exact (Rao, 1971)	$\tilde{\beta}_i$	$\bar{\beta}_i$	Exact (Rao, 1971)	$\tilde{\beta}_i$	$\bar{\beta}_i$	Exact (Rao, 1971)	$\tilde{\beta}_i$	$\bar{\beta}_i$
Panel A										
180°	1	1.839	1.837	1.838	1.769	1.770	1.773	1.647	1.654	1.659
(0.080)	2	5.305	5.310	5.312	4.778	4.773	4.786	4.176	4.177	4.173
	3	11.108	11.118	11.123	9.360	9.341	9.375	7.701	7.699	7.729
	4	19.006	19.022	19.031	14.841	14.818	14.869	11.676	11.686	11.709
270°	1	0.758	0.760	0.761	0.747	0.748	0.748	0.729	0.726	0.727
(0.053)	2	2.000	2.001	2.003	1.888	1.887	1.892	1.758	1.777	1.783
	3	4.406	4.408	4.414	3.997	3.993	4.006	3.624	3.597	3.610
	4	7.822	7.832	7.842	6.778	6.770	6.795	4.898	5.705	5.777
360°	1	0.438	0.438	0.439	0.433	0.434	0.434	0.424	0.426	0.427
(0.040)	2	0.952	0.952	0.9551	0.918	0.918	0.921	0.887	0.893	0.896
	3	2.137	2.139	2.144	2.005	2.005	2.012	1.892	1.893	1.901
	4	3.965	3.971	3.980	3.661	3.606	3.620	3.312	3.315	3.327
			$\tilde{\beta}_i^*$	$\bar{\beta}_i^*$		$\tilde{\beta}_i^*$	$\bar{\beta}_i^*$		$\tilde{\beta}_i^*$	$\bar{\beta}_i^*$
Panel B										
180°	1	1.839	1.837	1.837	1.769	1.770	1.772	1.647	1.654	1.657
(0.080)	2	5.305	5.310	5.307	4.778	4.772	4.781	4.176	4.150	4.168
	3	11.108	11.116	11.111	9.360	9.324	9.361	7.701	7.654	7.711
	4	19.006	19.016	19.010	14.841	14.715	14.829	11.676	11.533	11.661
270°	1	0.758	0.760	0.7605	0.747	0.748	0.748	0.729	0.726	0.727
(0.053)	2	2.000	2.001	2.000	1.888	1.887	1.889	1.758	1.776	1.779
	3	4.406	4.408	4.404	3.997	3.991	3.997	3.624	3.586	3.601
	4	7.822	7.830	7.824	6.778	6.756	6.776	4.898	5.668	5.773
360°	1	0.438	0.438	0.438	0.433	0.434	0.434	0.424	0.426	0.426
(0.040)	2	0.952	0.952	0.952	0.918	0.918	0.919	0.887	0.892	0.894
	3	2.137	2.139	2.137	2.005	2.004	2.006	1.892	1.891	1.895
	4	3.965	3.970	3.965	3.661	3.603	3.607	3.312	3.300	3.313

Note: $\tilde{\beta}_i$ and $\bar{\beta}_i$ with "consistent-mass" model and $\tilde{\beta}_i^*$ and $\bar{\beta}_i^*$ with "lumped-mass" model are obtained from CB and SB elements, respectively. $\bar{\alpha}$ is the total subtended angle and $\widetilde{S}_r$ is the slenderness ratio defined by $\widetilde{S}_r = [b/(R\bar{\alpha})](b/R)$.

notation β_i denote the values of β_i obtained using the curved beam (CB) elements and straight beam (SB) elements, respectively, while the right superscript "$*$" on β_i shown in Table 1(panel B) denotes the values of β_i obtained using lumped-mass model. In other words, the notation β_i (without superscript "$*$") denotes the values of β_i obtained using consistent-mass model (cf. Table 1(panel A)). From Table 1 one sees that: (i) The values of β_i ($i = 1$–4) obtained from SB element based on the consistent-mass model, $\bar{\beta}_i$, are very close to the corresponding ones obtained from the CB element based on the consistent-mass model, $\tilde{\beta}_i$, particularly those for the lowest three modes (i.e., $\bar{\beta}_i \approx \tilde{\beta}_i$); (ii) The values of β_i ($i = 1$–4) obtained from the SB element based on lumped-mass model, $\bar{\beta}_i^*$, are very close to the corresponding ones obtained from the CB element based on the lumped-mass model, $\tilde{\beta}_i^*$ (i.e., $\bar{\beta}_i^* \approx \tilde{\beta}_i^*$); (iii) The values of β_i ($i = 1$–4) obtained from either the SB element ($\bar{\beta}_i$ and $\bar{\beta}_i^*$) or the CB element ($\tilde{\beta}_i$ and $\tilde{\beta}_i^*$) are also very close to the corresponding exact solutions given by Rao (1971) as listed in columns 3, 6 and 9 of Table 1, respectively; (iv) The values of either $\tilde{\beta}_i$, $\bar{\beta}_i$, $\tilde{\beta}_i^*$ or $\bar{\beta}_i^*$ ($i = 1$–4), decrease with increasing the total subtended angle $\bar{\alpha}$; (v) The differences between the values of either $\tilde{\beta}_i$, $\bar{\beta}_i$, $\tilde{\beta}_i^*$ or $\bar{\beta}_i^*$ ($i = 1$–4) for the Timoshenko beams and the corresponding ones for the rotary (or Euler) beams decrease with decreasing the slenderness ratios $\widetilde{S}_r = [b/(R\bar{\alpha})](b/R)$. Based on all the above-mentioned reasonable results, it is believed that the theory presented and the computer programs developed for this paper should be available.

For a straight beam, the effects of rotary inertias and shear deformation are dependent upon the length ratio defined by $\overline{S}_r = b/L$ with L being the beam length. However, for a curved beam, the last effects are dependent upon both the arc-length ratio $b/(R\bar{\alpha})$ and thickness ratio b/R. Therefore, the slenderness ratio for a curved beam is defined by $\widetilde{S}_r = [b/(R\bar{\alpha})](b/R)$ in this paper.

8.3. Validation of forced vibration responses

To confirm the reliability of the presented theories regarding the forced vibration responses of a horizontally curved beam subjected to a moving load (cf. Fig. 6), the example given by Yang and Wu (2001) was solved using the CB elements incorporated with the consistent-mass models here. The curved beam was simply supported (i.e., $u_y = \psi_\theta = 0$) and the given data are: $a = 5$ m, $b = 1.8$ m, $\bar{\alpha} = 30° = \pi/6$ rad, $R = 45.84$ m, total arc length $L = R\bar{\alpha} = 24$ m, $E = 32.2 \times 10^9$ N/m^2, $v = 0.2$, $G = E/[2(1+v)] = 13.417 \times 10^9$ N/m^2, $k' = 0.833$, $I_x = ab^3/12 = 2.43$ m^4, $I_y = ba^3/12 = 18.75$ m^4, $J_\theta = I_x + I_y = 21.18$ m^4, $A = ab = 9$ m^2, $V_P = 40$ m/s, $P = 9.8 \times 29.9 \times 10^3$ N and damping ratio $\xi_d = 0$. It is noted that, to agree with Yang and Wu

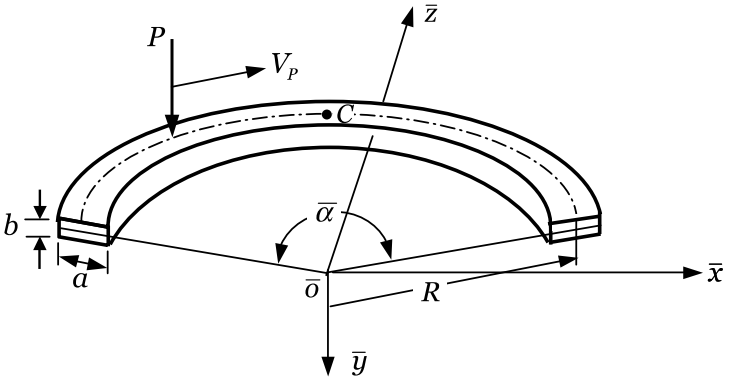

Fig. 6. Nomenclature for a horizontally curved beam subjected to a moving load P.

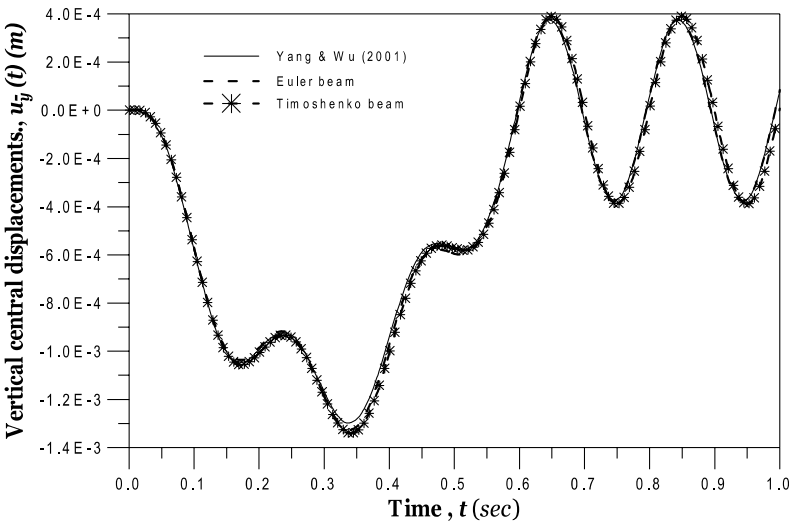

Fig. 7. Time histories of vertical displacements at the middle point C of the simply supported 30° horizontally curved beam subjected to a moving load with $P = 293{,}020$ N, $V_P = 40$ m/s and damping ratio $\xi_d = 0$ obtained from Yang and Wu (2001) (____) and from this paper: (—) for Euler beam; ($\cdots * \cdots$) for Timoshenko beam.

(2001), the values of I_x and J_θ are calculated with the classical simple formulas, $I_x = ab^3/12$, $I_y = a^3b/12$ and $J_\theta = I_x + I_y$, in this section and with Eqs. (3b) and (3c) throughout the paper.

The equations of motion for the forced vibrating system were solved with the Newmark direct integration method (Bathe, 1982) with time step $\Delta t = 0.001$ s. Fig. 7 shows the time histories of the vertical displacements at the middle point C of the curved beam, $u_{\bar{y}}(t)$. Where the solid line (—) was obtained from Yang and Wu (2001) and the dash line (– – –) and the dotted line with stars ($\cdots * \cdots$) were obtained from this paper based on the Euler beam theory and Timoshenko beam theory, respectively, using CB elements incorporated with the consistent-mass model. Closeness to each other between the three curves reveals the availability of the presented theories and the developed computer programs. Since the present curved beam is a "thin" beam with slenderness ratio $\widetilde{S}_r = [b/(R\bar{\alpha})](b/R) = 0.0029$, the effects of shear deformation and rotary inertias are negligible. This is the reason why the time history of the Euler beam is very close to that of the Timoshenko beam as shown in Fig. 7.

8.4. Effect of slenderness ratio ($\widetilde{S}_r$) on natural frequencies

From Table 1 one finds that the frequency parameters β_i ($i = 1$–4) of the Timoshenko beams are much smaller than the corresponding ones of the Eluer beams for the circular arc with subtended angle $\bar{\alpha} = 180°$, this is because the 180° circular arc is a "thick" beam with slenderness ratio $\widetilde{S}_r = [b/(R\bar{\alpha})](b/R) = 0.080$. However, for the arc with subtended angle $\bar{\alpha} = 360°$ the values of β_i ($i = 1$–4) for the Timoshenko beams are very close to the corresponding ones for the Eluer beams, because slenderness ratio of the 360° arc, $\widetilde{S}_r = 0.040$, is much smaller than that of the 180° arc. The circular arcs for Table 1 are "long" curved beams with subtended angle $\bar{\alpha} > 90°$, thus, this section studies the effect of slenderness ratio $\widetilde{S}_r$ on natural frequencies of a "short" curved beam with $\bar{\alpha} < 90°$, i.e., the simply supported 30° horizontally curved beam for Fig. 7. Here all dimensions of the curved beam are kept unchanged except that the size of the axial thickness (b) is enlarged from 1.8 to 3.6, 5.4, and 7.2 m, respectively. Table 2 shows the influence of slenderness ratio $\widetilde{S}_r$ on the lowest four frequency parameters, $\tilde{\beta}_i$ ($i = 1$–4), for the Euler beam, the rotary beam and the Timoshenko beam obtained from the CB elements incorporated with the consistent-mass

Table 2
The lowest four frequency parameters of the simply supported 30° horizontally curved beam, $\tilde{\beta}_i = \omega_i\sqrt{\rho AR^4/(EI_x)}$ ($i = 1$–4), obtained from CB elements incorporated with the "consistent-mass" model

Axial thickness b, m	$\bar{\alpha}$ ($\widetilde{S}_r$)	Mode no., i	Euler beam	Rotary beam	Timoshenko beam
1.8	30° (0.0029)	1	34.866	34.755	34.543
				0.318%	0.926%
		2	142.864	141.430	138.019
				1.003%	3.391%
		3	322.869	316.047	300.285
				2.112%	6.994%
		4	574.919	554.205	510.319
				3.602%	11.236%
3.6	30° (0.0118)	1	34.608	34.209	33.433
				1.152%	3.395%
		2	142.600	137.226	126.330
				3.768%	11.109%
		3	322.604	297.742	255.927
				7.706%	20.668%
		4	574.665	519.567	406.392
				9.587%	29.281%
5.4	30° (0.0265)	1	34.388	33.509	31.966
				2.556%	7.043%
		2	142.368	130.891	115.894
				8.061%	18.595%
		3	322.380	272.055	229.496
				15.610%	28.811%
		4	574.432	475.899	345.183
				17.153%	39.908%
7.2	30° (0.0472)	1	34.238	32.700	30.336
				4.492%	11.396%
		2	142.204	122.956	100.103
				13.535%	29.606%
		3	322.202	270.102	181.516
				16.169%	43.663%
		4	574.250	435.295	326.408
				24.197%	43.159%

Note: $\varepsilon\,\% = (\tilde{\beta}_{i\mathrm{Euler}} - \tilde{\beta}_{i\mathrm{X}}) \times 100\%/\tilde{\beta}_{i\mathrm{Euler}}$ (X = rotary, Timoshenko). $\bar{\alpha}$ is the total subtended angle and $\widetilde{S}_r$ is the slenderness ratio defined by

$$\widetilde{S}_r = [b/(R\bar{\alpha})](b/R).$$

model. It is seen that the effect of the slenderness ratio $\widetilde{S}_r$ on the current "short" circular arcs is the same as that on the "long" ones for Table 1: the values of $\tilde{\beta}_i$ ($i = 1$–4) for the Timoshenko beam are very close to the corresponding ones for the rotary (or Euler) beam if $\widetilde{S}_r < 0.0029$ and those for the Timoshenko beam are much smaller than the corresponding ones for the rotary (or Euler) beam if $\widetilde{S}_r > 0.0472$. The percentage differences (ε %) in Table 2 were determined from the formula: $\varepsilon\,\% = (\tilde{\beta}_{i\mathrm{Euler}} - \tilde{\beta}_{i\mathrm{X}}) \times 100\%/\tilde{\beta}_{i\mathrm{Euler}}$ with X = rotary and Timoshenko, and $\tilde{\beta}_{i\mathrm{Euler}}$ being the values of $\tilde{\beta}_i$ obtained from the Euler beams as shown in column 4 of Table 2.

From the final four rows of Table 1(panel A or B) one finds that the effects of shear deformation and rotary inertias on the lowest four natural frequencies of the "clamped–clamped" 360° curved beam (with slenderness ratio $\widetilde{S}_r = 0.040$) are small, however, this is not true for the "simply supported" 30° curved

beam (with slenderness ratio $\widetilde{S}_r = 0.0472$) as one may see from the final four rows of Table 2. It is believed that the last phenomenon is reasonable, because the modal displacements of a "clamped–clamped" beam are much smaller than those of a "simply supported" beam if their slenderness ratios are close to each other.

8.5. Effect of Slenderness Ratio ($\widetilde{S}_r$) on Forced Vibration Responses

In general, the influence of a factor on the forced vibration responses of a vibrating system will be similar to its influence on the frequency parameters of the same vibrating system. To confirm the last statement, the simply supported 30° horizontally curved beam for Fig. 7 and Table 2 with slenderness ratio $\widetilde{S}_r = 0.0472$ and subjected to the moving load with $P = 293{,}020$ N, $V_P = 40$ m/s, but damping ratio $\xi_d = 0.05$ is studied. Fig. 8. shows the time histories for the vertical displacements at the middle point C of the curved beam, where the solid line (—) is obtained from the Euler beam, the dashed line with triangles (–△–) is from the rotary beam and the dotted line with stars ($\cdots * \cdots$) is from the Timoshenko beam. In Fig. 7, the time history for the Euler beam is very close to that for the Timoshenko beam, but this is not true for the time histories shown in Fig. 8. This is because the slenderness ratio for Fig. 7 ($\widetilde{S}_r = 0.0029$) is much smaller than that for Fig. 8 ($\widetilde{S}_r = 0.0472$). In other words, for a "thin" beam (i.e., the one with small slenderness ratio) the frequency parameters and the forced vibration responses of the Euler beam or the rotary beam are very close to those of the Timoshenko beam, but for a "thick" beam (i.e., the one with large slenderness ratio) the frequency parameters and the forced vibration responses of the Euler beam or the rotary beam will be much different from those of the Timoshenko beam.

8.6. Dynamic responses of a hybrid curved beam due to a moving load

Fig. 9 shows the plane view of the hybrid curved beam studied. It is composed of one 120° curved beam segment and two identical straight beam segments. The given data for the curved beam are: $a = 0.1$ m, $b = 0.04$ m, $A = 4 \times 10^{-3}$ m^2, $R = 0.5$ m, $E = 18.4 \times 10^{10}$ N/m^2, $v = 0.27$, $G = E/[2(1+v)] = 7.244 \times 10^{10}$

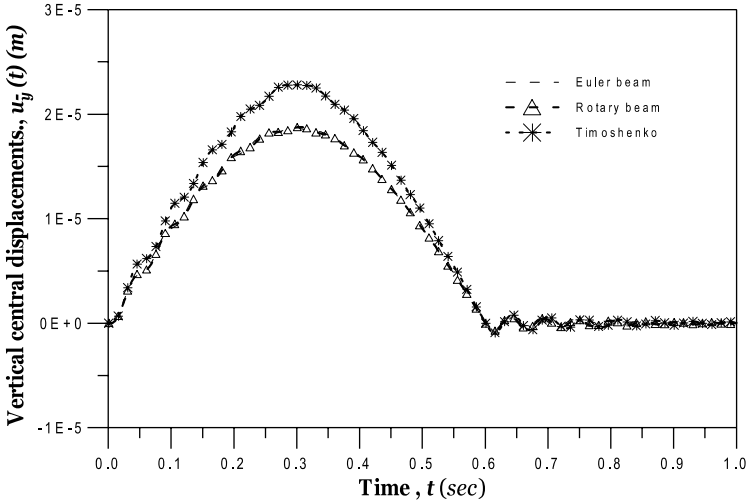

Fig. 8. Time histories of vertical displacements at middle point C of the simply supported 30° horizontally curved beam with slenderness ratio $\widetilde{S}_r = 0.0472$ and subjected to a moving load with $P = 293{,}020$ N, $V_P = 40$ m/s and damping ratio $\xi_d = 0.05$: (—) for Euler beam; (-△-) for rotary beam; ($\cdots * \cdots$) for Timoshenko beam.

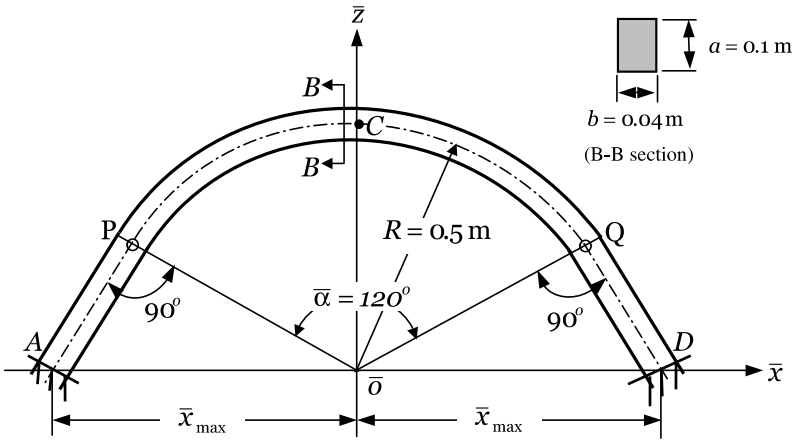

Fig. 9. Plane view for the clamped–clamped hybrid beam composed of one 120° circular beam segment and two identical straight beam segments with junctions P and Q simply supported.

Table 3
The lowest five natural frequencies of the clamped–clamped hybrid curved beam shown in Fig. 9, ω_i (rad/s)

Mode no., i	Natural frequencies, ω_i (rad/s)	
	S-C method	S-S method
1	810.748	810.542
2	2413.574	2413.634
3	4899.331	4900.895
4	6885.820	6886.443
5	8052.980	8053.395

N/m^2, $\rho = 7.69 \times 10^3$ kg/m^3, $k' = 0.833$. The cross-sections for the two straight beam segments are the same as those of the circular beam segment and the length for each of them is $R \tan 30° = 0.2887$ m.

Two techniques were used to solve the problem: the S-C method and the S-S method. The S-C method is a new approach with the straight parts of the hybrid beam modeled by the straight beam elements and the circular part modeled by the curved beam elements, while the S-S method is the conventional finite element method with both the straight parts and the circular part of the hybrid beam modeled by the straight beam elements. The lowest five natural frequencies of the hybrid curved beam, ω_i ($i = 1$–5), were shown in Table 3. From Table 3 one sees that the values of ω_i ($i = 1$–5) obtained from the S-C method are very close to the corresponding ones from the S-S method. Thus, the key points presented in Section 5 for the modification of property matrices of the conventional straight beam element will be correct.

If the hybrid curved beam is "at rest" at time $t = 0$ and is subjected to a moving load with magnitude $P = 50{,}000$ N and tangential speed $V_P = 0.5$ m/s moves from the left end A to right end B along the centerline of the hybrid beam (see Fig. 9), then the time histories for the vertical displacements at the middle point C of the hybrid beam were shown in Fig. 10. In which, the solid lines (—) denote the time histories obtained from the S-C method and the dashed lines (- - -) denote those obtained from the S-S method. Among the three solid lines and the three dashed lines, those without any attachments (— and - - -) were obtained from the Euler beam theory, those with triangles (–△– and -△-) from the rotary beam theory and those with star (–∗– and -∗-) from the Timoshenko beam theory. Since the present hybrid beam is a "thin" beam (with slenderness ratio $\widetilde{S}_r = [b/(R\bar{\alpha})](b/R) \approx 0.002$), its dynamic responses obtained from the Euler

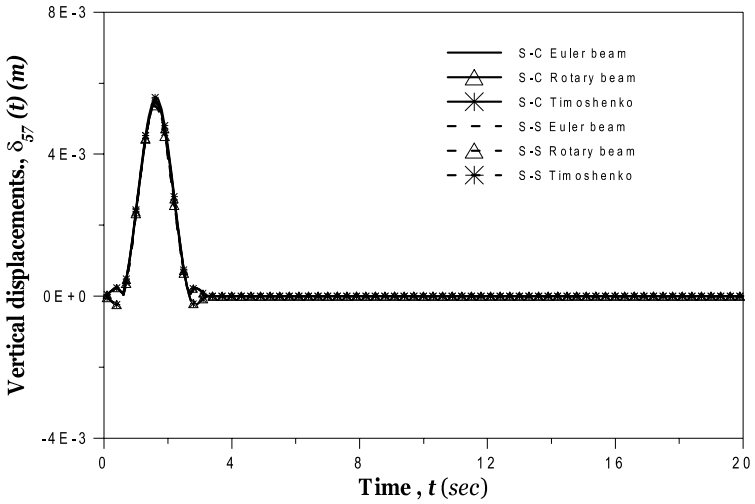

Fig. 10. The time histories for middle point C of the hybrid beam shown in Fig. 9 subjected to a moving load with magnitude $P = 50{,}000$ N and tangential speed $V_P = 0.5$ m/s along the centerline; obtained from the S-C method (—, –△–, –∗–); obtained from the S-S method (- - -, - -△- -, - -∗- -).

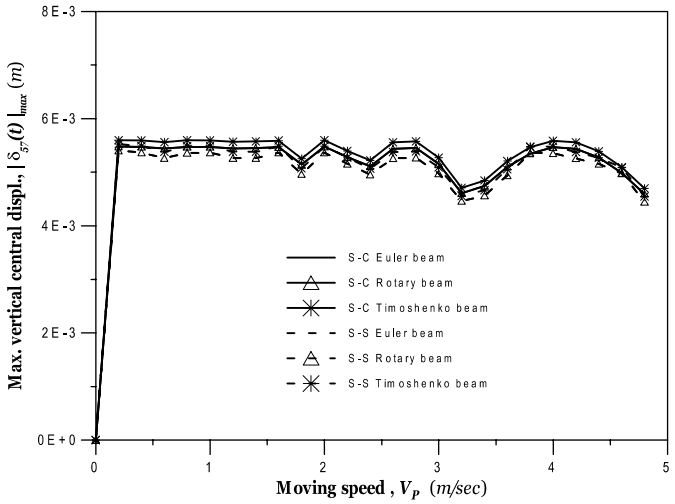

Fig. 11. Influence of moving speed (V_P) on the maximum vertical displacements at the middle point C of the hybrid beam subjected to a moving load with magnitude $P = 50{,}000$ N obtained from the S-C method (—, –△–, –∗–) and the S-S method (- - -, -△-,-∗-). The static deflection at the middle point C of the hybrid beam is $\delta_{st57} = 5.47 \times 10^{-3}$ m.

beam theory or the rotary beam theory are very close to those obtained from the Tiomshenko beam theory as shown in Fig. 10. From Fig. 10 one sees that the maximum vertical displacement at the middle point C of the hybrid beam occurs at the instant of time $t \approx 1.62$ s. The instantaneous distance of the moving load from the initial position, the left end A of the hybrid beam, is $s = V_P t = 0.5 \times 1.62 = 0.81$ m, which is near the middle point C of the hybrid beam. Therefore, the maximum vertical displacement at the middle point C of the hybrid beam due to a moving load will occurs at the instant of time that the moving load passing

through the middle point C. From Fig. 10 one also finds that the vertical displacement of the middle point C gradually increases when the moving load P moves towards C and gradually decreases when the moving load moves away from C. It is evident that all the last results agree with the actual situations.

The influence of the moving-load speed V_P on the maximum vertical central displacements of the hybrid beam was shown in Fig. 11. Where the legends for the six curves are exactly the same as those shown in Fig. 10. It is evident that the dynamic responses of the hybrid beam obtained from the S-C methods (denoted by the solid lines) are very close to those obtained from the S-S method (denoted by the dashed lines). The last result agrees with that obtained from Table 3 for the lowest five natural frequencies. In addition, the dynamic responses obtained from the Timoshenko beam theory are very close to those obtained from the rotary beam theory or the Euler beam theory. Since the static deflection at the middle point C of the hybrid beam is found to be $\delta_{st57} = 5.471 \times 10^{-3}$ m, dividing the ordinates of Fig. 11 by δ_{st57} will give the corresponding magnification factors for the hybrid beam.

9. Conclusions

1. If a beam with rotary inertias and shear deformation neglected is called the Euler beam, that with the effect of bending and torsional inertias considered is called the rotary beam, and that with the effects of both the rotary inertias and shear deformation considered is called the Timoshenko beam, then the stiffness matrix and mass matrix for the curved beam element and the straight beam element presented in this paper are available for the Euler (classical) curved beams, the rotary curved beams and the Timoshenko curved beams.

2. Using either the curved beam element or the straight beam element, the natural frequency parameters (β_r) obtained from the lumped-mass model are very close to the corresponding ones obtained from the consistent-mass model, thus, for simplicity, one may use the simple lumped mass matrix instead of the complex consistent mass matrix to perform the dynamic analysis of the curved beams.

3. For a curved beam with axial thickness b, total subtended angle $\bar{\alpha}$ and average radius of curvature R, the effects of rotary inertias and shear deformation are dependent upon both the arc-length ratio $b/(R\bar{\alpha})$ and thickness ratio b/R, thus, the slenderness ratio for a curved beam was defined by $\widetilde{S}_r = [b/(R\bar{\alpha})](b/R)$ in this paper. Numerical results reveal that the influence of slenderness ratio $\widetilde{S}_r$ on the free vibration responses of a curved beam is similar to that on the forced vibration responses, and for a "thin" curved beam (i.e., the one with small slenderness ratio, e.g., $\widetilde{S}_r < 0.0029$), the effects of rotary inertias and shear deformation are negligible. It is noted that, the slenderness ratio for a conventional straight beam is only dependent upon the length ratio and is defined by $\overline{S}_r = b/L$ with L being the beam length.

4. For a hybrid beam composed of curved and straight beam segments, if the technique modeling the straight parts of the hybrid beam by straight beam elements and the curved parts by curved beam elements is called the S-C method and that modeling all the hybrid beam by the conventional straight beam elements is called the S-S method, then either the S-C method or the S-S method may be used to predict the dynamic behaviors of the hybrid curved beam to achieve the satisfactory results.

5. When the S-C method is used to perform the dynamic analysis of a hybrid curved beam, appropriate modification in the property matrices of the conventional straight beam element is necessary. In such a case, the key points presented in Section 5 (cf. Fig. 2 also) will be beneficial.

Acknowledgements

This paper is part of the project under contract no. NSC90-2611-E-06-011. The authors acknowledge the financial support of the National Science Council, Republic of China.

Appendix A. Coefficients of Matrix $[\overline{H}]$

$$\overline{H}_{11} = A[\theta]_{\theta_1}^{\theta_2}$$

$$\overline{H}_{21} = \frac{C_{SO}A}{2}\left[\theta^2\right]_{\theta_1}^{\theta_2}$$

$$\overline{H}_{22} = \left[C_{SO}^2 A\left(\frac{\theta^3}{3}\right) + \frac{I_x}{R^2}\theta\right]_{\theta_1}^{\theta_2}$$

$$\overline{H}_{31} = -A[\cos\theta]_{\theta_1}^{\theta_2}$$

$$\overline{H}_{32} = \left[\left(C_{SO}A + \frac{I_x}{R^2}\right)\sin\theta - C_{SO}A\theta\cos\theta\right]_{\theta_1}^{\theta_2}$$

$$\overline{H}_{33} = \left[\left(A + \frac{I_x + J_\theta}{R^2}\right)\frac{\theta}{2} - \left(A - \frac{I_x - J_\theta}{R^2}\right)\frac{\sin\theta\cos\theta}{2}\right]_{\theta_1}^{\theta_2}$$

$$\overline{H}_{41} = A[\sin\theta]_{\theta_1}^{\theta_2}$$

$$\overline{H}_{42} = \left[\left(C_{SO}A + \frac{I_x}{R^2}\right)\cos\theta + C_{SO}A\theta\sin\theta\right]_{\theta_1}^{\theta_2}$$

$$\overline{H}_{43} = \frac{1}{2}\left[\left(A - \frac{I_x - J_\theta}{R^2}\right)\sin^2\theta\right]_{\theta_1}^{\theta_2}$$

$$\overline{H}_{44} = \left[\left(A + \frac{I_x + J_\theta}{R^2}\right)\frac{\theta}{2} + \left(A - \frac{I_x - J_\theta}{R^2}\right)\frac{\sin\theta\cos\theta}{2}\right]_{\theta_1}^{\theta_2}$$

$$\overline{H}_{51} = A[\sin\theta - \theta\cos\theta]_{\theta_1}^{\theta_2}$$

$$\overline{H}_{52} = \left[\left(2C_{SO}A + \frac{I_x}{R^2}\right)\theta\sin\theta - C_{SO}A\left(\theta^2 - 2\right)\cos\theta\right]_{\theta_1}^{\theta_2}$$

$$H_{53} = \left[\left(A + \frac{I_x + J_\theta}{R^2}\right)\frac{\theta^2}{4} - \left(A + \frac{J_\theta - I_x}{R^2}\right)\frac{\theta\sin 2\theta}{4} - \left(A + \frac{J_\theta - I_x}{R^2}\right)\frac{\cos 2\theta}{8} + \left(\frac{I_x - 2C_O J_\theta}{R^2}\right)\frac{\sin^2\theta}{2}\right]_{\theta_1}^{\theta_2}$$

$$H_{54} = \left[-\left(A + \frac{I_x + (1 + 4C_O)J_\theta}{R^2}\right)\frac{\theta}{4} + \left(A + \frac{J_\theta - I_x}{R^2}\right)\frac{\theta\sin^2\theta}{4} + \left(A + \frac{I_x + (1 - 4C_O)J_\theta}{R^2}\right)\frac{\sin\theta\cos\theta}{4}\right]_{\theta_1}^{\theta_2}$$

$$H_{55} = \left[\left(A+\frac{I_x+J_\theta}{R^2}\right)\frac{\theta^3}{6} - \left(A+\frac{J_\theta-I_x}{R^2}\right)\left(\frac{2\theta^2-1}{8}\right)\sin 2\theta - \left(A+\frac{J_\theta-I_x}{R^2}\right)\frac{\theta\cos 2\theta}{4} + \left(\frac{I_x-2C_OJ_\theta}{R^2}\right)\theta\sin^2\theta + \left(\frac{2C_OJ_\theta(1+2C_O)}{R^2}\right)\frac{\theta}{2} - \left(\frac{2C_OJ_\theta(1-2C_O)}{R^2}\right)\frac{\sin\theta\cos\theta}{2}\right]_{\theta_1}^{\theta_2}$$

$$\overline{H}_{61} = A[\cos\theta+\theta\sin\theta]_{\theta_1}^{\theta_2}$$

$$\overline{H}_{62} = \left[\left(2C_{SO}A+\frac{I_x}{R^2}\right)\theta\cos\theta + C_{SO}A\left(\theta^2-2\right)\sin\theta\right]_{\theta_1}^{\theta_2}$$

$$\overline{H}_{63} = \left[-\left(A-\frac{3I_x+(4C_O-1)J_\theta}{R^2}\right)\frac{\theta}{4} + \left(A-\frac{I_x-J_\theta}{R^2}\right)\frac{\theta\sin^2\theta}{2} + \left(A+\frac{I_x+(1-4C_O)J_\theta}{R^2}\right)\frac{\sin\theta\cos\theta}{4}\right]_{\theta_1}^{\theta_2}$$

$$H_{64} = \left[\left(A+\frac{I_x+J_\theta}{R^2}\right)\frac{\theta^2}{4} + \left(A+\frac{J_\theta-I_x}{R^2}\right)\frac{\theta\sin 2\theta}{4} + \left(A+\frac{J_\theta-I_x}{R^2}\right)\frac{\cos 2\theta}{8} + \left(\frac{2C_OJ_\theta-I_x}{R^2}\right)\frac{\sin^2\theta}{2}\right]_{\theta_1}^{\theta_2}$$

$$H_{65} = \left[\left(A+\frac{J_\theta-I_x}{R^2}\right)\frac{\theta^2\sin^2\theta}{2} + \left(\frac{I_x-4C_O^2J_\theta}{R^2}\right)\frac{\sin^2\theta}{2} - \left(A+\frac{J_\theta-I_x}{R^2}\right)\frac{\theta^2}{4} + \left(A+\frac{I_x+J_\theta(1-4C_O)}{R^2}\right)\left(\frac{\theta\sin 2\theta}{4}+\frac{\cos 2\theta}{8}\right)\right]_{\theta_1}^{\theta_2}$$

$$H_{66} = \left[\left(A+\frac{I_x+J_\theta}{R^2}\right)\frac{\theta^3}{6} + \left(A+\frac{J_\theta-I_x}{R^2}\right)\left(\frac{2\theta^2-1}{8}\right)\sin 2\theta + \left(A+\frac{J_\theta-I_x}{R^2}\right)\frac{\theta\cos 2\theta}{4} + \left(\frac{2C_OJ_\theta-I_x}{R^2}\right)\theta\sin^2\theta + \left(\frac{2C_OJ_\theta(2C_O-1)+2I_x}{R^2}\right)\frac{\theta}{2} + \left(\frac{4C_OJ_\theta(1-2C_O)}{R^2}\right)\frac{\sin\theta\cos\theta}{4}\right]_{\theta_1}^{\theta_2}$$

where

$$[f(\theta)]_{\theta_1}^{\theta_2} = f(\theta_2) - f(\theta_1)$$

References

Bathe, K.J., 1982. Finite Element Procedures in Engineering Analysis. Prentice-Hall, New Jersey.

Bickford, W.B., Maganty, S.P., 1986. On the out-of-plane vibrations of thick rings. J. Sound Vibrat. 108 (3), 503–507.

Chaudhuri, S.K., Shore, S., 1977. Dynamic analysis of horizontally curved I-girder bridge. J. Struct. Div., ASCE 103 (ST8), 1589–1604.

Davis, R., Henshel, R.D., Warburton, G.B., 1972a. Curved beam finite elements for coupled bending and torsional vibration. Earthquake Eng. Struct. Dynam. 1, 165–175.

Davis, R., Henshell, R.D., Warburton, G.B., 1972b. Discussion of 'effects of transverse shear and rotatory inertia on the coupled twist-bending vibrations of circular rings'. J. Sound Vibrat. 21 (2), 241–247.

Howson, W.P., Jemah, A.K., 1999. Exact out-of-plane natural frequencies of curved Timoshenko beams. J. Eng. Mech., ASCE 125 (1), 19–25.

Kawakami, M., Sakiyama, T., Matsuda, H., Morita, C., 1995. In-plane and out-of-plane free vibrations of curved beams with variable sections. J. Sound Vibrat. 187 (3), 381–401.

Kirkhope, J., 1976. Out-of-plane vibration of thick circular ring. J. Eng. Mech. Div., ASCE 102 (EM2), 239–247.

Lebeck, A.O., Knowlton, J.S., 1985. A finite element for three-dimensional deformation of a circular ring. Int. J. Numer. Meth. Eng. 21, 421–435.

Lee, B.K., Oh, S.J., Park, K.K., 2002. Free vibrations of shear deformable circular curved beams resting on elastic foundation. Int. J. Struct. Stability Dynam. 2 (1), 77–97.

Palaninathan, R., Chandrasekharan, P.S., 1985. Curved beam element stiffness matrix formulation. Comp. Struct. 21 (4), 663–669.

Przemieniecki, J.S., 1968. Theory of Matrix Structural Analysis. McGraw-Hill.

Rao, S.S., 1971. Effects of transverse shear and rotatory inertia on the coupled twist-bending vibrations of circular rings. J. Sound Vibrat. 16 (4), 551–566.

Silva, J.M.M., Urgueira, A.P.V., 1988. Out-of-plane dynamic response of curved beams—an analytical model. Int. J. Solid Struct. 24 (3), 271–284.

Wang, T.M., Nettleton, R.H., Keita, B., 1980. Natural frequencies for out-of-plane vibrations of continuous curved beams. J. Sound Vibrat. 68 (3), 427–436.

Wu, J.S., Chiang, L.K., 2003. Out-of-plane free vibrations of circular curved Timoshenko beams using the finite curved beam elements. Technical Report, Department of Naval Architecture and Marine Engineering, National Chen-Kung University, Tainan, Taiwan 701, Republic of China.

Yang, Y.B., Wu, C.M., 2001. Dynamic response of a horizontally curved beam subjected to vertical and horizontal moving loads. J. Sound Vibrat. 242 (3), 519–537.

Yoo, C.H., Fehrenbach, J.P., 1981. Natural frequencies of curved girders. J. Eng. Mech. Div., ASCE 107 (EM2), 339–354.